

Article

Modelling and Microstructural Aspects of Ultra-Thin Sheet Metal Bundle Cutting

Jarosław Kaczmarczyk ^{1,*}, Aleksandra Kozłowska ², Adam Grajcar ² and Sebastian Sławski ¹

¹ Institute of Theoretical and Applied Mechanics, Silesian University of Technology, 44-100 Gliwice, Poland; sebastian.slawski@polsl.pl

² Institute of Engineering Materials and Biomaterials, Silesian University of Technology, 44-100 Gliwice, Poland; aleksandra.kozłowska@polsl.pl (A.K.); adam.grajcar@polsl.pl (A.G.)

* Correspondence: jaroslaw.kaczmarczyk@polsl.pl; Tel.: +483-2237-2790

Received: 31 December 2018; Accepted: 29 January 2019; Published: 1 February 2019



Abstract: The results of numerical simulations of the cutting process obtained by means of the finite element method were studied in this work. The physical model of a bundle consisting of ultra-thin metal sheets was elaborated and then submitted to numerical calculations using the computer system LS-DYNA. Experimental investigations rely on observation of metallographic specimens of the surfaces being cut under a scanning electron microscope. The experimental data showing the microstructure of an ultra-thin metal bundle were the basis for the verification of the numerical results. It was found that the fracture area consists of two distinct zones. Morphological features of the brittle and ductile zones were identified. There are distinct differences between the front and back sides of the knife. The experimental investigations are in good agreement with the simulation results.

Keywords: steel sheet; cutting; finite element method; scanning electron microscope; plastic zone; brittle area; fracture

1. Introduction

In this paper the cutting problem of ultra-thin steel sheets arranged in bundles is considered. The sheets are made of C75S (carbon steel) cold rolled steel. The thickness of a single plate is 100 μm . The process of preparation of such thin sheets is complex and the cutting technology is also sophisticated. Cutting of bundles is more efficient compared to cutting individual sheets, because it enables the cutting of many sheets with a single cutting tool passage. The most frequently occurring defects are the bends of the cut sheet edges, burrs as well as defects in the form of vertical scratches. In order to improve the cutting process, numerical investigations were carried out concerning mainly the use of the finite element method for numerical simulation of cut sheet separation together with experimental research aimed at verifying the obtained results.

2. State of the Art

The cutting process of metals is the subject of interest of many researchers [1–4] as well as entrepreneurs and engineers working in the industrial sector. There are many interesting items in the literature regarding mainly machining [5–8], but much less attention is given to cover mechanical cutting of guillotines [9,10]. Different approaches are used for simulating failure and metal separation [11–13]. The most important issue is to select an appropriate FEM (finite element method) [14]. Machine deformation can also affect significantly the cutting process [15,16].

The cutting of a single sheet [9,17,18] is much simpler in comparison with cutting a stack of sheets. The smaller the number of sheets in the bundle the better the quality of the sheets cut in cross section [17]. By the good quality of sheets being cut, one means: low roughness of the sheets

in cross section, small number of defects in the shape of vertical craters, burrs that occur very rarely and insignificant edge bending. The best solution to achieve these goals is to avoid any kind of possible defects, but from the practical point of view it seems to be impossible because by nature the mentioned problems are often met in industry [19]. The only thing one can do is to improve the cutting process by changing the selected parameters that affect the process. Nowadays, it is rather difficult to eliminate entirely the negative causes of defects during the cutting process. It can be achieved by optimisation taking into account one criterion or many criteria [20–23] to minimise the chosen entity e.g., roughness, edge bending, burrs, vertical scratches in the shape of vertical craters, etc. Before optimisation one should be familiar with the mechanisms of the cutting process. Then one can influence many parameters of the cutting process in order to achieve the minimum roughness, minimum edge bending, the rare probability of occurrence of burrs and as well as vertical scratches. Hence, the main goal of this paper is better understanding of the mechanism of the cutting process. The physical models and the corresponding mathematical ones were elaborated in order to visualise the stresses and strains in elastic and plastic zones at the chosen time instances during cutting of the bundle of ultra-thin sheets made of C75S cold rolled high-strength steel. Next, the experimental investigations were taken into consideration to show the shape of separate sheets after cutting under large magnification. The problem with observation of the cutting process under a scanning electron microscope is because of watching the sheets only after cutting. It would be perfect to see the whole cutting process, but up to now there is no such sufficiently fast apparatus with the appropriate large chambers in which the whole industrial cutting machine could be placed. That is why numerical simulations using the finite element method applying the computer program LS-DYNA were adopted [24]. It is worth mentioning that using the finite element method one should remember that it is only an approximation of a small portion of reality. To obtain good results one needs to assume the proper number of elements. The number of elements cannot be too small or too large because the obtained results will suffer an error. The smaller the element the smaller the digits are describing its volume, mass, inertia etc. During numerical simulations the small digits are multiplied, divided etc. That is why serious problems with numerical round off to a certain number of significant digits can occur in the case of too small elements. Too large elements can produce an error also. So, the optimum size of elements cannot be either too large or too small [25–30].

It was found out that in practice solution difficulties usually arise only when the finite element discretization is very fine, and for this reason the condition of infinite stresses under concentrated load is frequently ignored. Much finer discretization would lead to stress singularities at the point where the tip of the blade touches the sheet being cut. Additional errors might be caused also by computer approximation of the very small floating-point digits because the numbers are processed by round off. However, in general the finer the mesh the better the results (small errors) but the time of calculations increases. Therefore the balance between accuracy and time of computations should be established. If the size of the elements in the model is too large the time of computations decreases but the value of errors increases. This is caused usually by assumed linear shape function and the number of nodes. In the current work the proper size of the mesh was established on the basis of experiment and the numerical calculations were verified with experimental data.

The cutting of a bundle of metal sheets is the field of interest of such authors as Gasiorek et al. [4]. Their paper presents numerical modelling of the guillotine cutting process of sheet aluminium bundles. A finite element method with a smoothed particle hydrodynamics approach was coupled to simulate the cutting process. Experimental results of the cutting were presented for the validation purposes. The measured force characteristics in all numerical simulations and experiment were compared. The mentioned researchers focused on investigations of deformations and plastic strains.

It can be concluded that cutting on guillotines is a niche subject appearing in the literature rather sporadically when the problems related to machining processes have been thoroughly discussed. Research concerning cutting of single sheets using a guillotine shear can be found in Ref. [10]. The

authors formulated physical models and corresponding to them mathematical ones using the computer program LS-DYNA [24].

The authors of the current paper covered such topics as mechanisms of the cutting process, plastic strains, reduced Huber–Mises stresses as well as the microstructure of the surfaces of sheets being cut.

In a previous work [9] the authors investigated the relationships between the cutting depth and the values of reduced Huber–Mises stresses for one sheet. In the current study, the model of mechanism of sheet separation using two thin sheets forming a bundle, is presented. The microstructural aspects of the cutting process are also addressed. Moreover, the differences in cutting behaviour between the front part of the cutting tool and the back part are identified.

3. Methodology

To achieve the goal of the study the following methodology was applied:

- to conduct fast changing dynamical calculations, the finite element method and the computer system LS-DYNA (LSTC, Livermore, CA, USA) were deployed;
- to obtain the experimental verification of the cutting, microstructural observations of fracture surfaces were performed, the SEM images were obtained using a Zeiss SUPRA 25 (Carl Zeiss AG, Jena, Germany) scanning microscope operating at 20 kV under two different magnifications: 400× and 800×;
- the final stage concerns the comparison of the numerical simulations with the experimental results.

3.1. Material

To conduct the numerical investigations of the cutting process, a bilinear material model for the bundle of sheets made of C75S high-strength steel was assumed. The detailed data are collected together and shown in Table 1. Such a material model is very popular in the literature because on one hand it describes the elastic-plastic behaviour and on the other hand it is relatively simple. The bilinear material model (Figure 1) consists of two lines which describe the double relationship, respectively, the elastic one which is modelled by a straight line that starts from the origin of the Cartesian coordinate system of the stress–strain relation and the plastic one modelled by the second line which starts at the yield point and describes the plastic reinforcement. Despite the assumed bilinear material model being simple it describes the nonlinear behaviour between stress and strain.

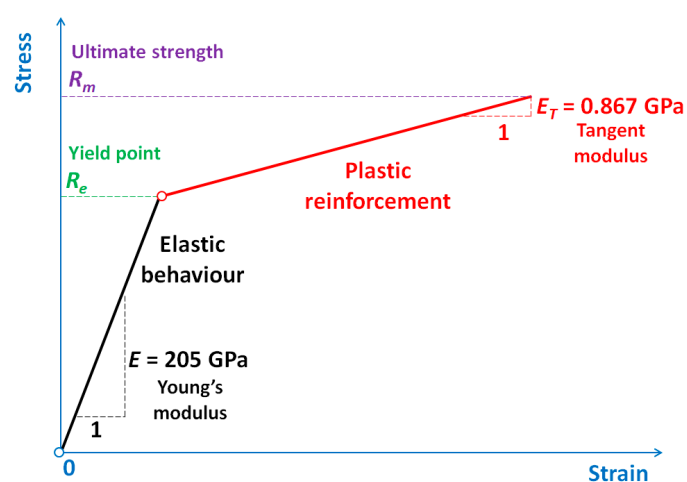


Figure 1. Bilinear material model.

Table 1. Material properties for steel sheets being cut.

No	Name of the Material Properties	Symbol	Value
1.	Young's modulus	E	205 GPa
2.	Poisson's ratio	ν	0.28
3.	Kirchhoff's modulus	G	80 GPa
4.	Tangent modulus	E_T	0.867 GPa
5.	Failure strain	ϵ_f	0.15
6.	Yield stress	R_e	0.51 GPa
7.	Ultimate tensile strength	R_m	0.64 GPa

3.2. Physical Model of the Bundle of Sheets

In order to model the numerical cutting process, the physical model of the process was elaborated. It contains such parts as:

- cutting tool,
- pressure beam,
- bundle of sheets which consists of two separate metal sheets being cut,
- worktable.

All mentioned elements were modelled as rigid except the bundle of sheets which was modelled as deformable. This problem is focused on sheets being cut and on the quality of the cut surfaces understood as the smallest edge bending possible, burrs and vertical scratches in the shape of craters. The contact between the earlier mentioned working surfaces of all parts are taken into consideration. The unilateral constraints are imposed on the nodes that are in mutual contact during cutting i.e., between (Figures 2 and 3):

- the rigid cutting tool and the first deformable sheet,
- the rigid cutting tool and the second deformable sheet,
- the rigid pressure beam and the first deformable sheet,
- the first deformable sheet and the second deformable sheet,
- the second deformable sheet and the rigid worktable.

The models of Coulomb's and Moren's friction laws are taken into consideration. The static and kinetic coefficients of friction for all working surfaces in contact are assumed as for steel, respectively:

- static coefficient of friction $\mu_s = 0.22$,
- kinetic coefficient of friction $\mu_k = 0.11$.

The presented physical model (Figure 2) is divided into finite coplanar rectangular elements with four nodes (Figure 3). One node has two degrees of freedom (x and y translation). During modelling of the cutting process, the plane state of strain was applied [31]. Individual parts were divided into finite elements and nodes (Table 2). The size of the finite element of the sheet being cut is 0.02 mm horizontally and 0.01 mm vertically. The proposed element size was chosen on the basis of experiment as a compromise between the number of elements and the time consumption needed for the geometrically as well as the materially nonlinear fast changing dynamic cutting problem with cracking.

Table 2. Information about parts discretized into finite elements and nodes.

No	Name of the Part	Kind of Part	Number of Nodes	Number of Elements
1.	Cutting tool (knife)	Rigid	112	90
2.	First metal sheet being cut	Deformable	572	500
3.	Second metal sheet being cut	Deformable	572	500
4.	Pressure beam	Rigid	546	500
5.	Worktable	Rigid	1071	1000
Total number			2873	2590

The physical model of the sheet metal cutting process is shown in Figure 2. On a motionless perfectly rigid table the sheets being cut are placed and then they are pressed from the top using a perfectly rigid pressure beam made in the form of a wedge with convergence 1:30. In this work it is assumed that the cutting tool blade has an apex angle $\alpha = 30^\circ$ and the gap between the cutting tool and the pressure beam is 0.1 mm. The unilateral constraints in the form of so-called contact were imposed on the surfaces of the sheets being cut, worktable, pressure beam and cutting tool. The contact is based on the condition of impenetrability, namely the condition that two bodies cannot interpenetrate.

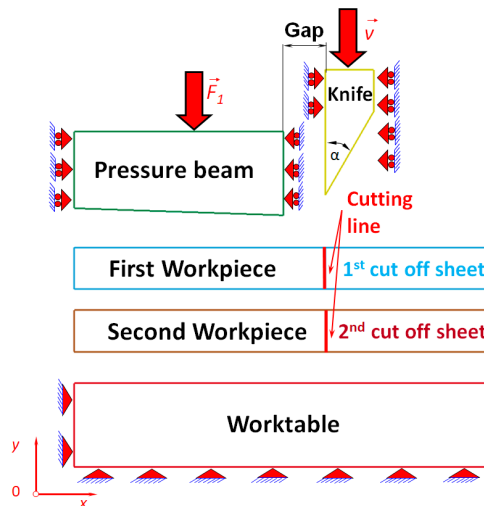


Figure 2. Physical model of a bundle consisting of two sheets being cut.

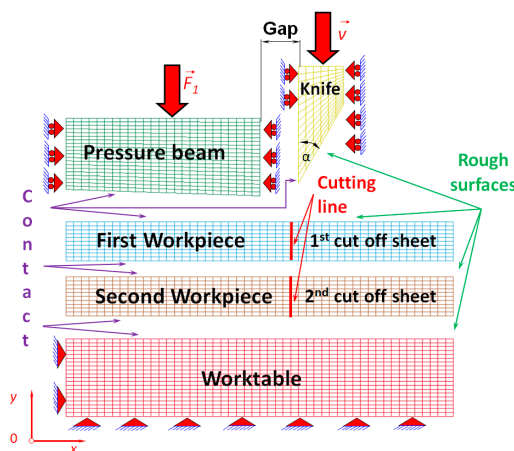


Figure 3. Mesh of the physical model of a bundle being cut.

To simulate the cutting process the failure model was applied. It consists of the separation of the nodes belonging to the cutting line (Figure 3). The nodes are defined as separable in the case when

the reduced Huber–Mises strain at the closest node to the tip of the blade of a cutting tool approaches the equivalent value of strain equal to 0.15. The mentioned value of strain corresponds to the rupture during the experimental uniaxial tensile test. If the reduced Huber–Mises strain is higher than 0.15 the node which is closest to the tip of the blade is separated into two independent nodes allowing the cutting tool to penetrate into the sheet being cut. In the case when the reduced Huber–Mises strain in the sheet is less than the equivalent value of strain (0.15), then the node which is closest to the tip of the blade is not separated. So it is left as a single node which means that further penetration is impossible because the mentioned node is not separated into two nodes and the cutting process stops at this point (node).

In order to carry out the numerical simulation of a cutting process, the nonlinear incremental differential equation of dynamical equilibrium taking into account the phenomena occurring in mutual contact between bodies should be applied [32]:

$$\begin{bmatrix} \mathbf{M} & \mathbf{0} \\ \mathbf{0} & \mathbf{0} \end{bmatrix} \begin{bmatrix} {}^{t+\Delta t}\Delta\ddot{\mathbf{u}}^{(i)} \\ 0 \end{bmatrix} + \begin{bmatrix} \mathbf{C} & \mathbf{0} \\ \mathbf{0} & \mathbf{0} \end{bmatrix} \begin{bmatrix} {}^{t+\Delta t}\Delta\dot{\mathbf{u}}^{(i)} \\ 0 \end{bmatrix} + \left\{ \begin{bmatrix} {}^{t+\Delta t}\mathbf{K}^{(i-1)} & \mathbf{0} \\ \mathbf{0} & \mathbf{0} \end{bmatrix} + [{}^{t+\Delta t}\mathbf{K}_c^{(i-1)}] \right\} \begin{bmatrix} {}^{t+\Delta t}\Delta\mathbf{u}^{(i)} \\ {}^{t+\Delta t}\Delta\lambda_k^{(i)} \end{bmatrix} = \begin{bmatrix} {}^{t+\Delta t}\mathbf{R} \\ \mathbf{0} \end{bmatrix} - \begin{bmatrix} \mathbf{M} & \mathbf{0} \\ \mathbf{0} & \mathbf{0} \end{bmatrix} \begin{bmatrix} {}^{t+\Delta t}\ddot{\mathbf{u}}^{(i-1)} \\ 0 \end{bmatrix} - \begin{bmatrix} \mathbf{C} & \mathbf{0} \\ \mathbf{0} & \mathbf{0} \end{bmatrix} \begin{bmatrix} {}^{t+\Delta t}\dot{\mathbf{u}}^{(i-1)} \\ 0 \end{bmatrix} - \begin{bmatrix} {}^{t+\Delta t}\mathbf{F}^{(i-1)} \\ \mathbf{0} \end{bmatrix} + \begin{bmatrix} {}^{t+\Delta t}\mathbf{R}_c^{(i-1)} \\ {}^{t+\Delta t}\Delta_k^{(i-1)} \end{bmatrix} \quad (1)$$

where:

- \mathbf{M}, \mathbf{C} —mass and damping matrices, respectively,
- ${}^{t+\Delta t}\mathbf{K}^{(i-1)}$ —tangent stiffness matrix including the material and geometric nonlinearities after iteration $(i-1)$,
- ${}^{t+\Delta t}\mathbf{K}_c^{(i-1)}$ —contact matrix after iteration $(i-1)$,
- ${}^{t+\Delta t}\mathbf{R}$ —vector of externally applied forces at time $t+\Delta t$,
- ${}^{t+\Delta t}\mathbf{F}^{(i-1)}$ —vector of nodal point forces after iteration $(i-1)$,
- ${}^{t+\Delta t}\mathbf{R}_c^{(i-1)}$ —vector of contact forces after iteration $(i-1)$,
- ${}^{t+\Delta t}\Delta_k^{(i-1)}$ —vector of material overlaps at contactor nodes after iteration $(i-1)$,
- ${}^{t+\Delta t}\Delta\mathbf{u}^{(i)}, {}^{t+\Delta t}\Delta\dot{\mathbf{u}}^{(i)}, {}^{t+\Delta t}\Delta\ddot{\mathbf{u}}^{(i)}$ —vectors of incremental displacements, velocities and accelerations respectively in iteration (i) ,
- ${}^{t+\Delta t}\Delta\lambda_k^{(i)}$ —vector of Lagrange multipliers in iteration (i) ,
- ${}^{t+\Delta t}\dot{\mathbf{u}}^{(i-1)}, {}^{t+\Delta t}\ddot{\mathbf{u}}^{(i-1)}$ —vector of velocities and accelerations respectively after iteration $(i-1)$.

In the successive stage Equation (1) is converted into a formula enabling direct integration of the considered dynamic problem using the computer system LS-DYNA.

The rupture in metal sheets being cut is described by the following equation:

$$\text{if } \varepsilon \geq \varepsilon_f \text{—node separation belonging to the cutting line takes place,} \quad (2)$$

$$\text{if } \varepsilon < \varepsilon_f \text{—no separation possible in nodes belonging to the cutting line,} \quad (3)$$

where: ε —reduced Huber–Mises strain, ε_f —failure strain.

3.3. Microscopic Investigations

Observations of fracture surface of 1st (top) and 2nd (bottom) sheets located in the bundle were carried out to determinate the rupture mode. This part of research was done on the basis of SEM images obtained by using Zeiss SUPRA 25 (Carl Zeiss AG, Jena, Germany) scanning microscope operating at 20 kV under two different magnifications: 400× and 800×. The details of the fracture were observed at the front and the back of the cutting tool.

4. Results and Discussion

The research is composed of the three following stages:

- the numerical simulations concerning the cutting process of a bundle of sheets,
- the experimental investigations consisting of a series of microstructural images obtained by means of a scanning electron microscope (SEM),
- the comparison of the numerical and experimental results.

4.1. Numerical Simulations

The bundle consisting of two sheets was analysed. The numerical calculations were carried out using the finite element method and computer system LS-DYNA which is a general-purpose finite element program capable of simulating complex real world problems. It is used by the automobile, aerospace, construction, military, manufacturing, and bioengineering industries. This program is optimized for shared and distributed memory Unix, Linux, and Windows based platforms. The code's origins lie in highly nonlinear, transient dynamic finite element analysis using explicit time integration. LS-DYNA capabilities include [24]: nonlinear dynamics, rigid body dynamics, normal modes, thermal analysis, fluid analysis, etc. The simulations were performed at the Silesian University of Technology using the computer cluster Ziemowit (<http://www.ziemowit.hpc.polsl.pl>). The cutting process begins at the moment at which the pressure beam starts moving slowly from zero to maximum speed ($\vartheta_{\max} = 0.012$ mm/s), then moves with constant maximum speed and next slows down imperceptibly until its speed approaches zero. Following this, the pressure beam touches the top of the bundle (Figures 4–7) and compresses the sheets with a small force a priori assumed and treated as negligibly small compared with the force produced by the knife during cutting. The small force guarantees the cutting of the bundle without any shifting of the sheets being cut. At the moment when the pressure beam stops, the cutting tool starts traveling from zero to maximum speed ($\vartheta_{\max} = 0.022$ mm/s) and then moves with constant maximum speed and starts cutting the bundle of sheets. It should be mentioned that the tip of the blade of a cutting tool travels parallel to the worktable. The cutting tool first cuts the top sheet in the bundle and after that it starts cutting the final sheet, then it stops at the worktable and goes back to the original position and the cutting process repeats itself.

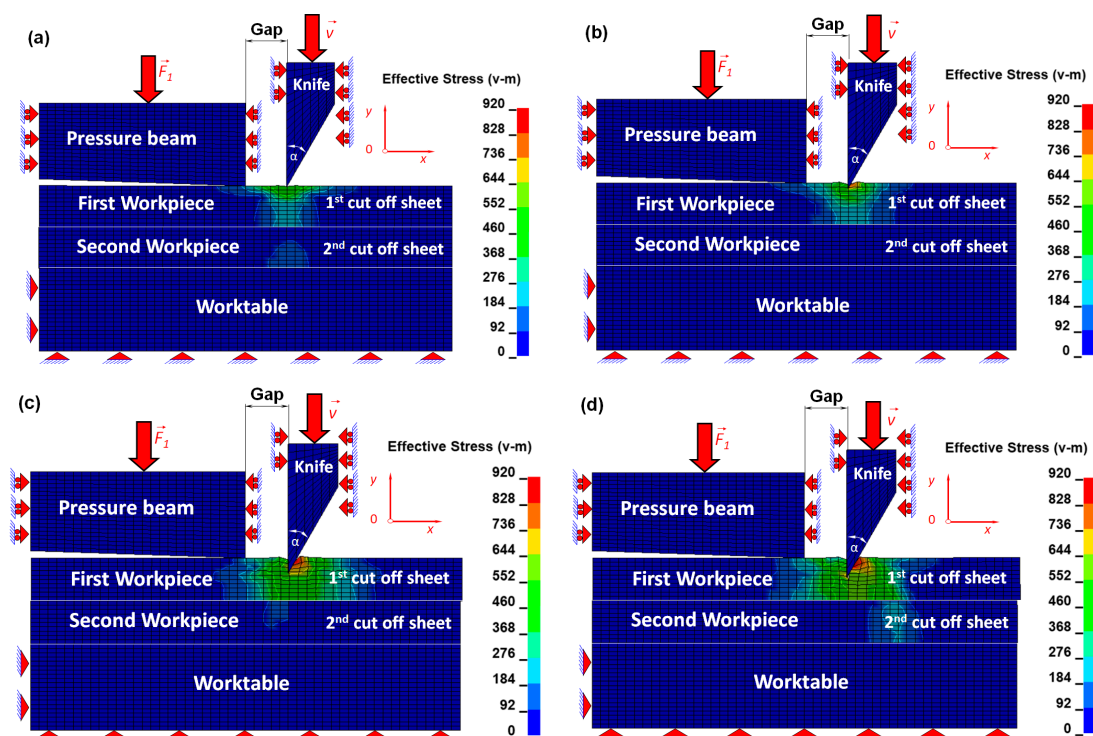


Figure 4. Cont.

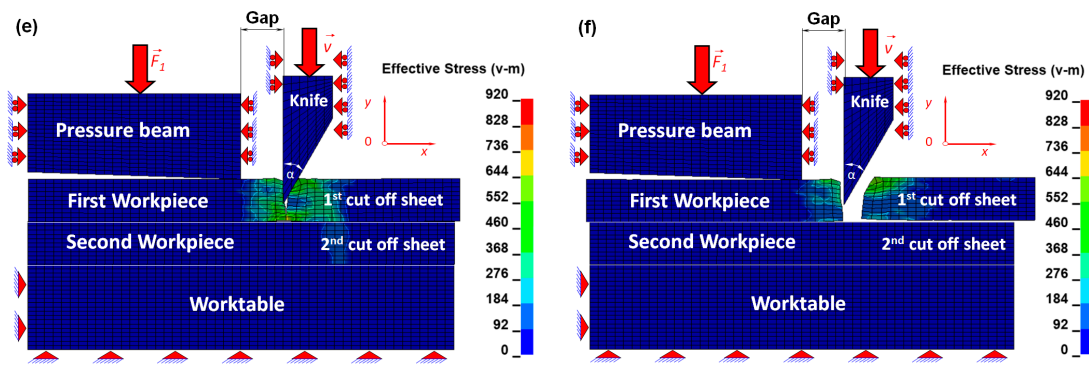


Figure 4. Huber–Mises stresses in the first sheet being cut for the following time instances: (a) $t = 3$ s, (b) $t = 3.5$ s, (c) $t = 4.5$ s, (d) $t = 5$ s, (e) $t = 5.55$ s, (f) $t = 5.56$ s. The visualisation of stresses for the next sheet being cut is continued in the next figure.

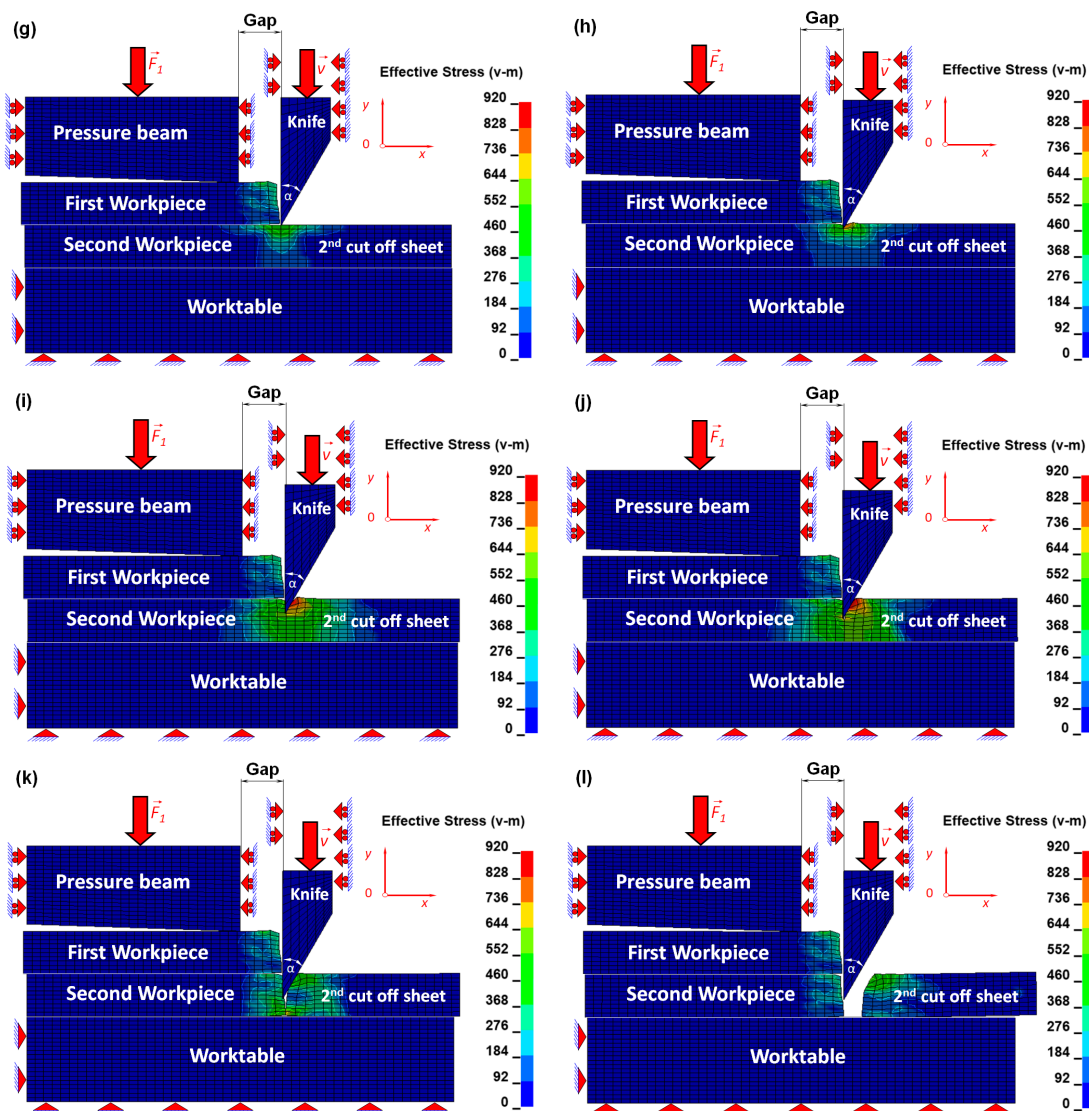


Figure 5. Huber–Mises stresses in the second sheet being cut for the following time instances: (g) $t = 7.5$ s, (h) $t = 8$ s, (i) $t = 9$ s, (j) $t = 9.5$ s, (k) $t = 10.1$ s, (l) $t = 10.11$ s (continuation of Figure 4). The visualisation of stresses for the previous sheet being cut is presented in the previous figure.

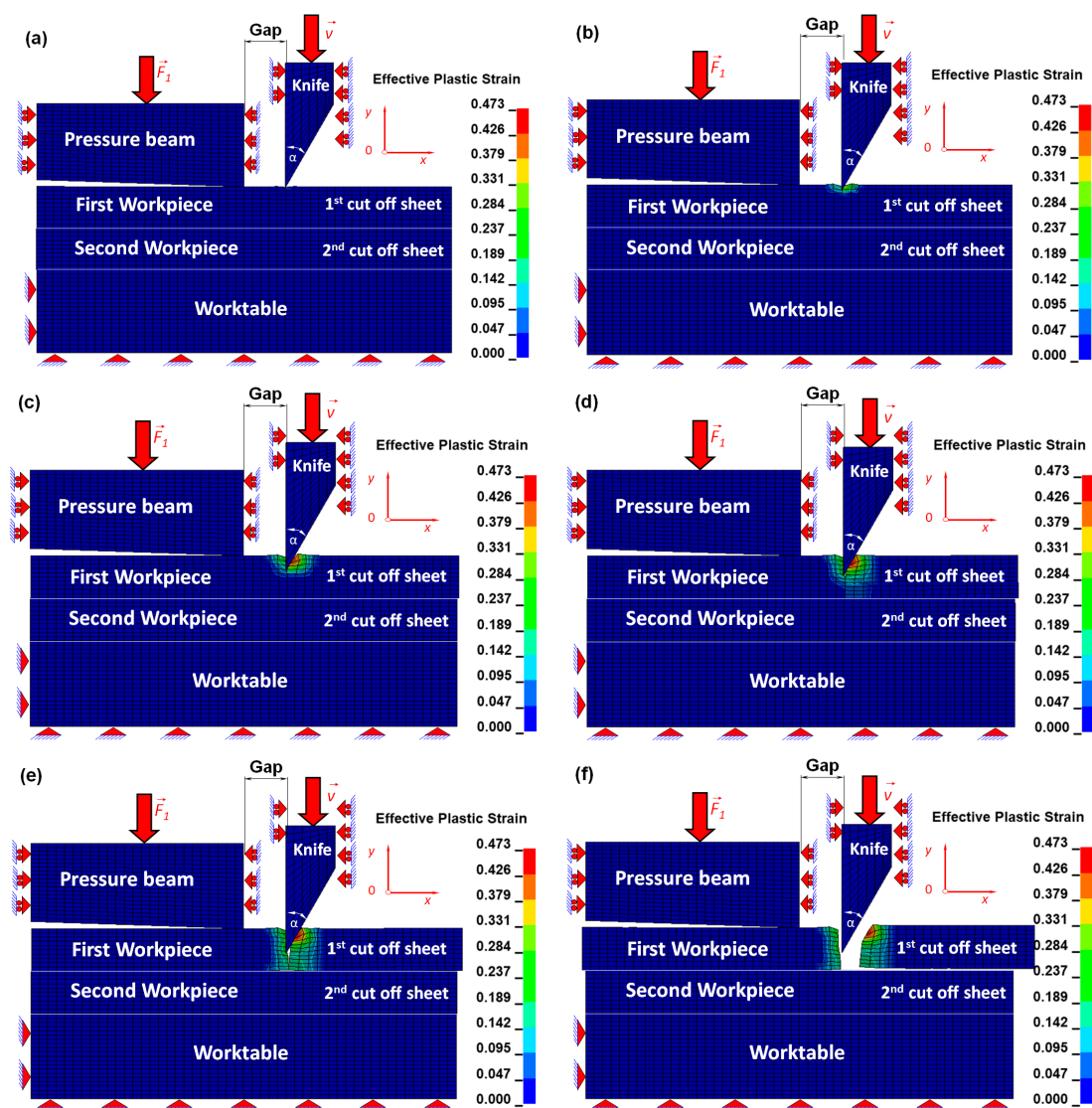


Figure 6. Effective plastic strains in the first sheet being cut for the following time instances: (a) $t = 3$ s, (b) $t = 3.5$ s, (c) $t = 4.5$ s, (d) $t = 5$ s, (e) $t = 5.55$ s, (f) $t = 5.56$ s. The effective plastic strains in the next sheet being cut are shown in the next figure.

During cutting in the first stage, the knife travels with constant speed downwards and touches the first top sheet being cut and starts pressing it and forming the elastic zone of the reduced Huber–Mises stresses (Figure 4a) and corresponding to it the equivalent Huber–Mises plastic strains (Figure 6a). So the reduced Huber–Mises stresses and strains grow from zero to the maximum values which correspond to the elastic limit. Since the cutting tool moves farther into the first sheet being cut, the stresses and strains exceed the elastic limit and start creating a plastic region close to the tip of the blade of the cutting tool (Figures 4b and 6b). The C75S steel begins to reinforce and finally the stresses and strains are so high that the material cannot withstand it anymore and so loses its continuity. Then the tip of the blade of the cutting tool penetrates into the first top sheet being cut and begins to shear it causing a ductile fracture as consequence. The sheet is being cut by separating it plastically (Figures 4c and 6c). The separation is possible since the early mentioned failure model was additionally adopted to enable the cutting process to be continued which consisted of the nodes being split up. The numerical simulations show that from the very beginning of cutting which starts at the top of each sheet until circa 1/3 of the height of the sheet being cut measured from its top downwards, the ductile fracture caused by shearing suddenly changes into brittle fracture caused by the tensile state of the stresses

which begins to dominate instead of shearing after exceeding the early mentioned 1/3 of the height of each sheet (Figure 4e,f and Figure 6e,f).

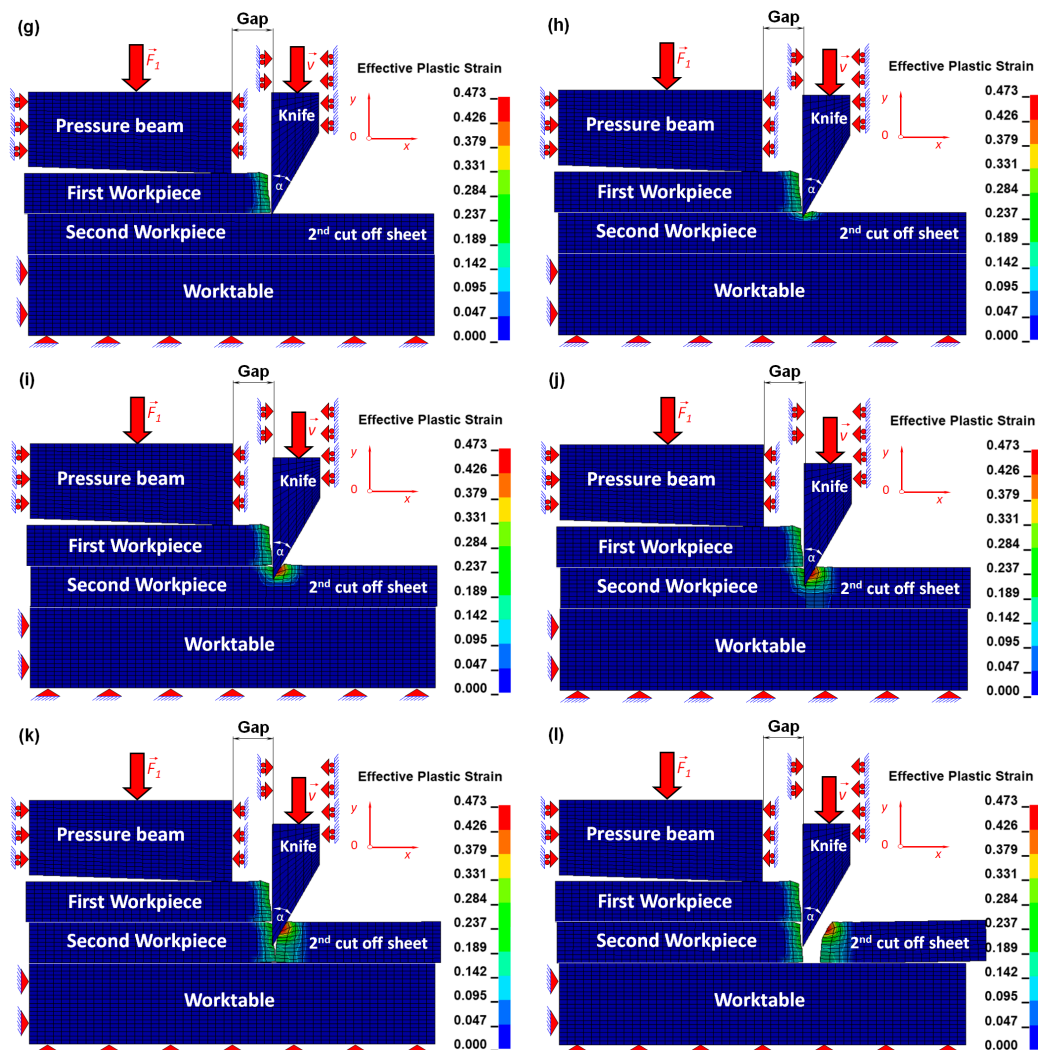


Figure 7. Effective plastic strains in the second sheet being cut for the following time instances: (g) $t = 7.5$ s, (h) $t = 8$ s, (i) $t = 9$ s, (j) $t = 9.5$ s, (k) $t = 10.1$ s, (l) $t = 10.11$ s (continuation of Figure 6). The effective plastic strains in the previous sheet being cut are shown in the previous figure.

The final stage of cutting is very interesting because it is connected with brittle cracking produced by tensile stresses. The described phenomenon is very similar to the experimental uniaxial tensile test. At the end of the stretching test, a neck is formed and cracking appears. This experimental tensile test is similar to the cracking observed during cutting of the sheet in the case where the tip of the blade penetrates into the sheet being cut at a height bigger than 1/3 of the height of the sheet. The cut surface is smooth, without burrs and vertical scratches. Such cut surfaces are required because they are fine unlike those induced by shearing accompanied by many defects. So, the only problem is the first stage concerning the shearing. It takes place from zero to circa 1/3 of the height of the sheet measured from its top downwards. During the shearing edge bending, scratches and large plastic zones are formed. On such cut surfaces there are many defects which are not desired (Figure 4a–c, Figure 5g–i, Figures 6a–c and 7g–i). The more sheets in a bundle, the more numerous are the defects. The sheet with the most defects is always the last one at the bottom. This work deals with only two sheets in a bundle but it is enough to prove numerically as well as experimentally that plastic deformations are more severe during the cutting of the last bottom sheet in a bundle (Figure 4c,d, Figure 5i,j, Figure 6c,d

and Figure 7i,j). The elastic and plastic zones during cutting of the second sheet are similar to the first one.

The only difference is that the bottom sheet is more severely plastically deformed. Comparing these two plastic zones in the two sheets being cut one can state that the second sheet is more deformed so the plastic strains are slightly higher. The second stage concerning the sheet being cut from 1/3 of the height to the whole height of the second sheet (Figure 5k,l and Figure 7k,l) is very similar to the same stage concerning the cutting of the first sheet (Figure 4e,f and Figure 6e,f). These stages are highly desired from a theoretical as well as practical point of view since a good quality of sheets being cut is highly sought after. On these cut surfaces where the brittle fracture occurs there are no burrs or vertical scratches in the shape of craters, etc.

4.2. Microscopic Details

The sheet metal bundle cutting process leads to the occurrence of two types of fracture. There is a substantial difference in the fracture character when comparing the back side and front side of the cutting tool (Figure 8). The presence of a fracture consisting of plastic and brittle parts in the zone located at the back of the cutting tool was observed. The ductile zone is always located in the upper part of the observed cross section, whereas the brittle zone occurs in its lower part (Figure 8a,c). The boundary between the ductile and brittle zones is located at a 1/3 of the sheet height measured from the top downwards independent of the place in the bundle.

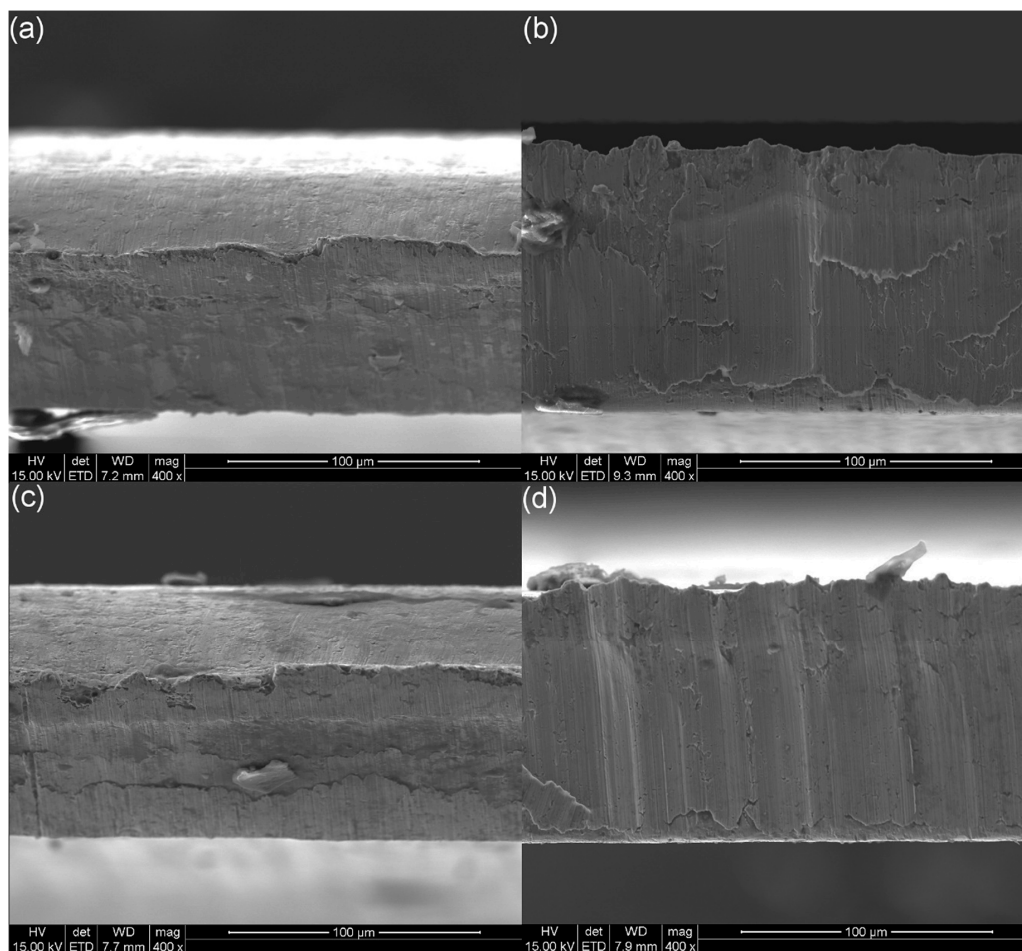


Figure 8. Cross sections of the steel sheets being cut depending on the localization of the observed surface: top sheet (a,b) and bottom sheet (c,d) at the back side of the cutting tool (a,c) and at the front side of the cutting tool (b,d) mag. 400×.

The plastic zone is characterized by a dimple mode of rupture. Most of the observed dimples are characterized by an oval shape. Moreover, some of them have a spherical shape. The dimples are characterized by various sizes. Most of them are relatively small due to the presence of numerous nucleating sites, which are activated during the deformation process. The micro-voids are closely located and they coalesce before they have an opportunity to grow to a larger size [33]. The lower part of the samples shows typical brittle fracture. Numerous brittle walls can be observed (Figure 9a,c) but no dimples were detected.

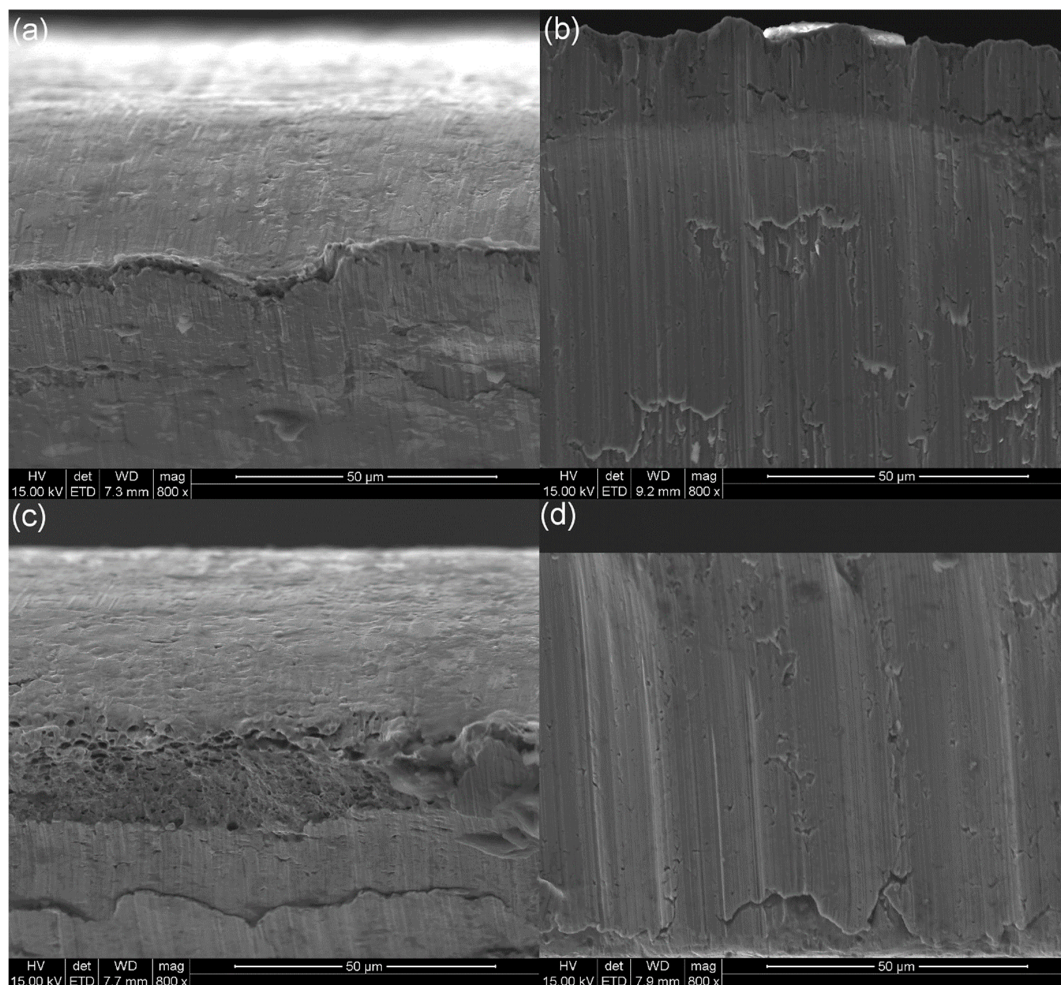


Figure 9. Details of the surface fracture of the steel sheets being cut depending on the localization of the observed surface: top sheet (a,b) and bottom sheet (c,d) at the back side of the cutting tool (a,c) and at the front side of the cutting tool (b,d) mag. 800×.

The cut surfaces located at the front of the cutting tool are characterized by the different nature of fracture in comparison to the surfaces located at the back side of the cutting tool. In this case, the observed cross sections are homogenous (Figure 8b,d). The typical features of brittle fracture are observed. The decohesion of all the steel sheets occurred without plastic deformation. The presence of irregular shear planes and numerous scratches are visible (Figure 9b,d) as well as some cracks.

There are no big differences when comparing the top and bottom sheets (Figure 8). However, one can see that the sheet located at the bottom of the bundle is more heavily affected by the cutting process.

4.3. Comparison of the Numerical and Experimental Investigations

The elaborated physical and mathematical models of the cutting process were the basis to carry out numerical simulations taking into account the failure model which corresponds to all nodes that

belong to the cutting line (Figure 3). Experimental verification using a scanning electron microscope was carried out. At the final stage the numerical as well as the experimental results were juxtaposed. This comparison is presented in Figure 10 and shows that the plastic region of sheets being cut begins from zero to 1/3 of the sheet height measured from the top of each sheet downwards. The plastic zone is slightly larger in the bottom sheet (Figure 10c,d). It might be explained by taking into account the friction which resists the impending motion of the cutting tool. During cutting of the first sheet, the friction force occurs only between the top sheet being cut and the cutting tool (Figures 4 and 6) whereas during cutting of the second sheet the friction force occurs not only between the bottom sheet being cut and the cutting tool but also between the mentioned cutting tool and the cut off top sheet which is on the left side between the pressure beam and the bottom sheet (Figures 5 and 7). That is why the conditions of cutting of the bottom sheet are slightly more severe than the conditions of cutting of the top sheet. Evidence that the second sheet being cut works in slightly heavier conditions comes from the graphs presenting the internal energy accumulated during cutting in both sheets (Figure 11) and for each sheet successively (Figure 12).

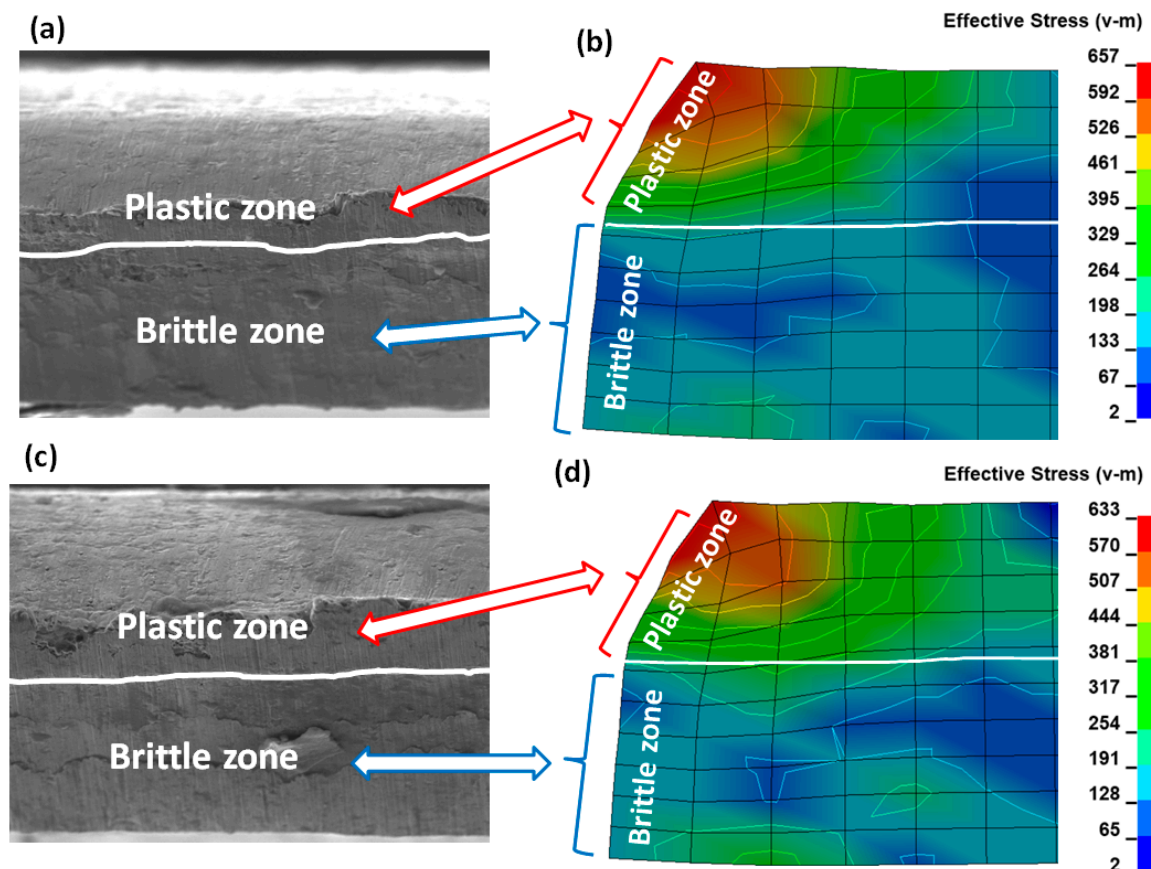


Figure 10. Comparison of the experimental and numerical results.

A similar comparison analysis was conducted by Bohdal [10], who investigated the cutting process of a single sheet being cut using a bench shear. The cutting process was simulated by means of the FEM-SPH model and was compared with the experimental data using recorded images from a high-speed camera. The experiment shows good agreement in the depth angle and the burr height with the numerical simulations. From the obtained results it can be seen that the fracture process becomes less steady and progresses in a non-uniform manner in some locations along the shearing line. An analysis of the state of stress, strain and fracture mechanisms of the material was presented. This approach of the author concerns shearing using bench shears however, in the current paper the cutting

process of ultra-thin metal sheets arranged in a bundle deals mainly with shearing but stretching as well.

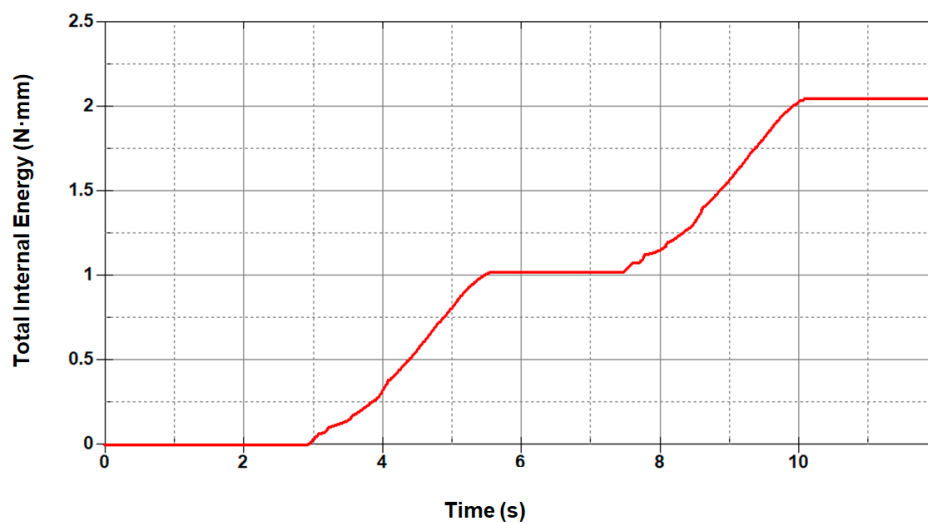


Figure 11. Total internal energy in both sheets being cut versus time.

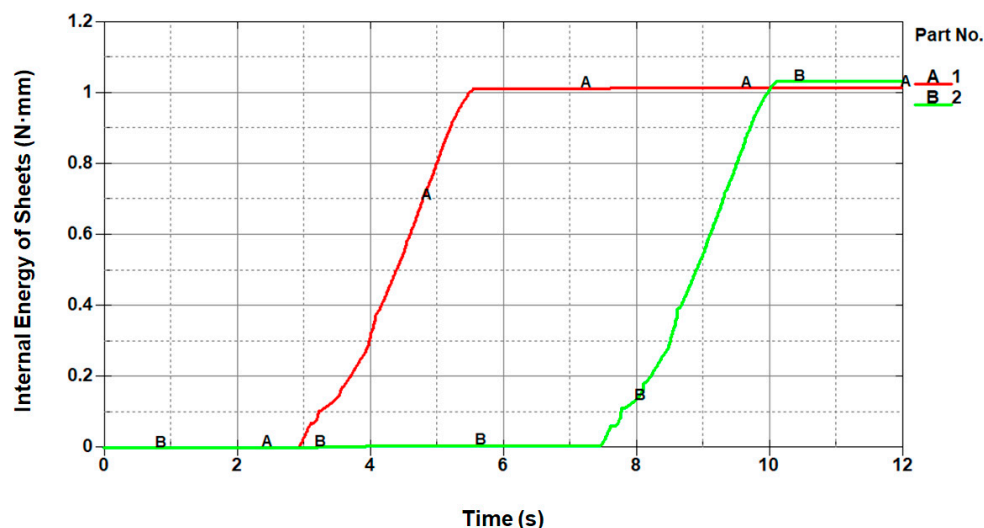


Figure 12. Internal energy for separated sheets being cut versus time: (A 1)—in the first sheet, (B 2)—in the second sheet.

5. Conclusions

In this paper the cutting problem was analysed for better understanding of the mechanisms involved. The cutting process is characterised by fast change of physical phenomena such as displacements, strains, stresses, etc. versus time and an additional problem constitutes the excessive speed of the process which prevents observation in detail by the unaided eye. That is why the physical model and corresponding to it the mathematical model of the cutting process were elaborated here. Next, numerical simulation using the finite element method and adopting the computer system LS-DYNA was performed in order to present the mechanism of the cutting process of sheets in a bundle. The elastic and plastic zones as well as the ductile and brittle fractures that occur during cutting at selected time intervals are presented. Experimental investigation was also carried out by observation of the steel sheets after cutting under a scanning electron microscope. The numerical and experimental results were compared with each other.

During study of the fast changing cutting process the following conclusions were drawn:

- the maximum stresses and the plastic strains obtained in the numerical simulations are mainly concentrated in sheets being cut close to the tip of the blade of a cutting tool,
- the maximum reduced Huber–Mises stresses in the first stage of cutting are higher than the yield point and that is why sheets being cut cannot withstand it with the result that ductile fracture occurs at a height from zero to circa 1/3 of the height of the sheet being cut measured from the top of the sheets downwards. In this particular ductile zone shearing dominates, justified on the base of numerical as well as experimental data,
- the maximum reduced Huber–Mises stresses in the final stage of cutting are higher even than the ultimate strength which occurs at a height larger than circa 1/3 of the height of the sheets being cut, measured from the top of the sheets downwards. The steel sheet being cut in this particular zone cannot withstand it and brittle fracture occurs because instead of shearing, stretching dominates implied on the basis of numerical simulations and verified by experiment,
- on the basis of SEM imaging it can be stated that ductile fracture is accompanied by many defects like burrs, vertical scratches, higher roughness, larger edge bending, etc.,
- brittle fracture has no significant defects and is characterised by a smooth surface in the cross section of the sheets being cut, observed under the scanning electron microscope.

Author Contributions: Conceptualization, J.K.; Data curation, J.K.; Formal analysis, J.K.; Funding acquisition, J.K.; Investigation, A.K., A.G. and S.S.; Methodology, J.K.; Software, J.K. and S.S.; Validation, J.K. and A.G.; Visualization, A.K.; Writing—original draft, J.K.; Writing—review and editing, A.K., A.G. and S.S.

Funding: This work was financially supported by statutory funds from the Faculty of Mechanical Engineering of Silesian University of Technology in 2018.

Acknowledgments: Numerical calculations were carried out using the computer cluster Ziemowit (<http://www.ziemowit.hpc.polsl.pl>) funded by the Silesian BIO-FARMA project No. POIG.02.01.00-00-166/08 in the Computational Biology and Bioinformatics Laboratory of the Biotechnology Centre in the Silesian University of Technology.

Conflicts of Interest: The authors declare no conflict of interest.

References

1. Arslanov, M.Z. A polynomial algorithm for one problem of guillotine cutting. *Oper. Res. Lett.* **2007**, *35*, 636–644. [[CrossRef](#)]
2. Alvarez-Valdes, R.; Parajon, A.; Tamarit, J.M. A tabu search algorithm for large-scale guillotine (un)constrained two-d imensional cutting problems. *Comput. Oper. Res.* **2002**, *29*, 925–947. [[CrossRef](#)]
3. Tiwari, S.; Chakraborti, N. Multi-objective optimization of a two-dimensional cutting problem using genetic algorithms. *J. Mater. Process. Technol.* **2006**, *173*, 384–393. [[CrossRef](#)]
4. Gasiorek, D.; Baranowski, P.; Malachowski, J.; Mazurkiewicz, L.; Wiercigroch, M. Modelling of guillotine cutting of multi-layered aluminum sheets. *J. Manuf. Process.* **2018**, *34*, 374–388. [[CrossRef](#)]
5. Nouari, M.; Makich, H. On the Physics of Machining Titanium Alloys: Interactions between Cutting Parameters, Microstructure and Tool Wear. *Metals* **2014**, *4*, 335–338. [[CrossRef](#)]
6. Razak, N.H.; Chen, Z.W.; Pasang, T. Effects of Increasing Feed Rate on Tool Deterioration and Cutting Force during and End Milling of 718Plus Superalloy Using Cemented Tungsten Carbide Tool. *Metals* **2017**, *7*, 441. [[CrossRef](#)]
7. Koklu, U.; Basmaci, G. Evaluation of Tool Path Strategy and Cooling Condition Effects on the Cutting Force and Surface Quality in Micromilling Operations. *Metals* **2017**, *7*, 426. [[CrossRef](#)]
8. Haddag, B.; Atlati, S.; Nouari, M.; Moufki, A. Dry Machining Aeronautical Aluminum Alloy AA2024-T351: Analysis of Cutting Forces, Chip Segmentation and Built-Up Edge Formation. *Metals* **2016**, *6*, 197. [[CrossRef](#)]
9. Kaczmarczyk, J.; Grajcar, A. Numerical Simulation and Experimental Investigation of Cold-Rolled Steel Cutting. *Materials* **2018**, *11*, 1263. [[CrossRef](#)] [[PubMed](#)]
10. Bohdal, Ł. Application of a SPH Coupled FEM Method for Simulation of Trimming of Aluminum Autobody Sheet. *Acta Mech. Autom.* **2016**, *10*, 56–61. [[CrossRef](#)]
11. Fedeliński, P.; Górski, R.; Czyż, T.; Dziaekiewicz, G.; Ptaszny, J. Analysis of Effective Properties of Materials by Using the Boundary Element Method. *Arch. Mech.* **2017**, *66*, 19–35.

12. Paggi, M. Crack Propagation in Honeycomb Cellular Materials: A Computational Approach. *Metals* **2012**, *2*, 65–78. [[CrossRef](#)]
13. Perez, N. *Fracture Mechanics*; Kluwer Academic Publishers: Boston, MA, USA, 2004.
14. González, H.; Pereira, O.; Fernández-Valdivielso, A.; López de Lacalle, L.N.; Calleja, A. Comparison of Flank Super Abrasive Machining vs. Flank Milling on Inconel[®] 718 Surfaces. *Materials* **2018**, *11*, 1638.
15. Del Pozo, D.; López de Lacalle, L.N.; López, J.M.; Hernández, A. Prediction of Press/Die Deformation for an Accurate Manufacturing of Drawing Dies. *Int. J. Adv. Manuf. Technol.* **2008**, *37*, 649–656. [[CrossRef](#)]
16. Lamikiz, A.; López de Lacalle, L.N.; Sanchez, J.A.; Bravo, U. Calculation of the Specific Cutting Coefficients and Geometrical Aspects in Sculptured Surface Machining. *Mach. Sci. Technol.* **2005**, *9*, 411–436. [[CrossRef](#)]
17. Kaczmarczyk, J. Numerical Simulations of Preliminary State of Stress in Bundles of Metal Sheets on the Guillotine. *Arch. Mater. Sci. Eng.* **2017**, *85*, 14–23. [[CrossRef](#)]
18. Kaczmarczyk, J.; Gasiorek, D.; Mezyk, A.; Skibniewski, A. Connection Between the Defect Shape and Stresses which Cause it in the Bundle of Sheets Being Cut on Guillotines. *Model. Optim. Phys. Syst.* **2007**, *6*, 81–84.
19. Show, M.C. *Metal Cutting Principles*; Oxford University Press: New York, NY, USA, 2005.
20. Bhatti, M.A. *Practical Optimization Methods*; Springer-Verlag Inc.: New York, NY, USA, 2000.
21. Rothwell, A. *Optimisation Methods in Structural Design*; Springer International Publishing AG: Delft, The Netherlands, 2017.
22. Goldberg, D.E. *Genetic Algorithms in Search, Optimization, and Machine Learning*; Addison-Wesley Publishing Company, Inc.: New York, NY, USA, 1989.
23. Michalewicz, Z. *Genetic Algorithms + Data Structures = Evolution Programs*; Springer: Berlin/Heidelberg, Germany, 1996.
24. *LS-DYNA Keyword User's Manual*; Livermore Software Technology Corporation: Livermore, CA, USA, 2017.
25. Bathe, K.J.; Chaudhary, A. A Solution Method for Planar and Axisymmetric Contact Problems. *Int. J. Numer. Method Eng.* **1985**, *21*, 65–88. [[CrossRef](#)]
26. Belytschko, T.; Liu, W.K.; Moran, B.; Elkhodary, K.I. *Nonlinear Finite Elements for Continua and Structure*; John Wiley & Sons, Ltd.: Southern Gate, CA, USA, 2014.
27. Fish, J.; Belytschko, T.A. *First Course in Finite Elements*; John Wiley & Sons, Ltd.: Southern Gate, CA, USA, 2007.
28. Mohammadi, S. *Discontinuum Mechanics Using Finite and Discrete Elements*; WIT Press Southampton: Boston, MA, USA, 2003.
29. Hughes, T.J.R. *The Finite Element Method. Linear Static and Dynamic Finite Element Analysis*; Manufactured in the United States by RR Donnelley: Chicago, IL, USA, 2016.
30. Zienkiewicz, O.C.; Taylor, R.L. *The Finite Element Method, Solid Mechanics*; Butterworth-Heinemann: Oxford, UK, 2000.
31. Timoshenko, S.P.; Goodier, J.N. *Theory of Elasticity*; McGraw-Hill Education: New York, NY, USA, 2017.
32. Chaudhary, A.B.; Bathe, K.J. A Solution Method for Static and Dynamic Analysis of Three—Dimensional Contact Problems with Friction. *Comput. Struct.* **1986**, *24*, 855–873. [[CrossRef](#)]
33. ASM Handbook. *Volume 12: Fractography*; ASM International: Cleveland, OH, USA, 1987.



© 2019 by the authors. Licensee MDPI, Basel, Switzerland. This article is an open access article distributed under the terms and conditions of the Creative Commons Attribution (CC BY) license (<http://creativecommons.org/licenses/by/4.0/>).